Heliyon 10 (2024) e39403

Contents lists available at ScienceDirect

Heliyon

journal homepage: www.cell.com/heliyon

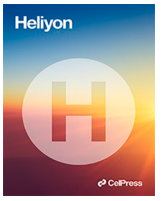

Research article

Study on the protective effect of flavonoids extracted from Jatropha curcas leaves against radiation damage in mice

Qinling Li *, Dan He, Yang He

Institute of Medical Technology, Sichuan College of Traditional Chinese Medicine, Mianyang, 621000, China

ARTICLE INFO

Keywords:
Jatropha curas leaves
Flavonoids extracted
Radiation damage
Immune functions
Hematopoietic functions

ABSTRACT

The primary objective of this study was to evaluate the radioprotective effects of Flavonoids Extracted from Jatropha curcas Leaves (FEL) and to elucidate the underlying protective mechanisms against radiation damage. Six monomers of the FEL were analyzed using Ultra Performance Liquid Chromatography (UPLC). The results indicate that FEL increases the survival rate of mice and promotes the recovery of organs damaged by ^{60}Co γ-rays to their normal appearance, through mechanisms that include the enhancement of immune and hematopoietic functions in vivo. In vitro studies suggest that the molecular mechanism by which FEL mitigates radiation damage involves the reduction of DNA damage and mutations. These findings indicate that FEL could be effective in alleviating radiation-induced injuries.

1. Introduction

With the ongoing advancement of industrialization, there is an increase in the incidence of ionizing radiation damage, radiation-induced oxidative stress, and the release of toxic substances. Radiation is a significant factor contributing to various forms of damage, leading to oxidative stress, dysfunction of the hematopoietic system, genetic mutations, and immune system impairment, ultimately resulting in a substantial decline in the immune response to disease [1]. Consequently, it is essential to protect humans from high doses of radiation. Currently, various chemical and biological agents are available for the prevention and treatment of radiation damage; however, they frequently lead to a range of side effects [2]. As a result, researchers are increasingly investigating natural products with anti-radiation properties [3–7]. Flavonoids, active compounds found in many Chinese herbal medicines, exhibit anti-inflammatory, analgesic, immune-regulatory, anti-tumor, and anti-radiation effects. Due to their low toxicity and cost-effectiveness, natural products containing flavonoids have garnered significant attention from researchers [8].

Jatropha (*Jatropha curcas* L.) is a member of the Euphorbiaceae family and thrives in tropical and subtropical regions. In China, its distribution is primarily concentrated in the provinces of Yunnan, Guizhou, Guangdong, Guangxi, Sichuan, Hainan, Taiwan, and several other areas. The seeds of Jatropha curcas are notable for their high oil content and excellent oil quality, thus holding significant value in industrial and medicinal applications [9]. Current research has identified nine distinct flavonoids isolated from various parts of Jatropha curcas, including the seeds, skin, stem, leaf, and root. Among these, the stem, root, and leaf demonstrate higher flavonoid content, with percentages of 0.42 %, 3.05 %, and 4.87 %, respectively. Notably, the leaves contain the highest concentration of flavonoids [10,11].

This study investigates how FEL mitigates the risk of radiation-related diseases. The findings reveal that the underlying mechanism

* Corresponding author.
E-mail address: lqlwwg2017@163.com (Q. Li).

https://doi.org/10.1016/j.heliyon.2024.e39403
Received 1 July 2024; Received in revised form 15 September 2024; Accepted 14 October 2024
Available online 15 October 2024

of this effect involves the enhancement of immune function and a reduction in chromosomal damage, ultimately providing protection against radiation-induced harm.

2. Materials and methods

2.1. Experimental plant

Fresh Jatropha leaves from Yuanmou County in Yunnan Province were collected and allowed to dry naturally (Fig. 1). Following this, the dried leaves were ground using a medicinal grinder and passed through a 40-mesh sieve to obtain finely processed samples. The samples were stored in a refrigerator at 4 °C until the experiments were conducted.

2.2. Preparation of flavonoids from the sample

The samples were pulverized using an electric grinder, and the resulting fine powder was defatted with ligarine in a Soxhlet apparatus. The defatted portion was removed, dried, and subjected to two extractions with 80 % ethanol. The solvents were evaporated under vacuum until dry, and the resulting residue was diluted in distilled water. After filtration to separate the precipitate, the remaining solution underwent further separation on an adsorptive resin column (ZTC-5, Tianjin, China). Elution was performed with water, 60 % ethanol, and 95 % ethanol to yield three fractions. The 60 % ethanol fraction was dried under vacuum, recrystallized with ethanol, and yielded a yellow powder containing the FEL. The structure of the compound was determined via ultraviolet, mass spectrometry, ^{1}H and ^{13}C NMR spectra.

2.3. UPLC diagram

The chemical profile of the FEL extract was analyzed using UPLC. The analysis was conducted with the ACQUITY UPLC system manufactured by Waters, a United States-based company. A bonded phase silica gel column with octadecylsilane chemistry (Waters ACQUITY UPLC BEH C_{18}, 1.7 μm) was utilized, featuring dimensions of 15 cm in length and 2.1 mm × 150 mm in volume. The extract underwent gradient elution with a mixture of acetonitrile and 1 % glacial acetic acid. The elution consisted of the following successive concentrations: 88 % acetonitrile (0.00 min), 82 % acetonitrile (10.00 min), 70 % acetonitrile (42.00 min), 65 % acetonitrile (50.00 min), 60 % acetonitrile (65.00 min), and 0 % acetonitrile (70.00 min). The detection wavelength was set at 266 nm, and the flow rate was maintained at 0.4 mL/min. The column temperature was kept at 40 °C, and a sample injection volume of 2 μL was used.

Accurately weigh out suitable amounts of 6 flavonoid standard substances, and dissolve them in methanol to prepare a standard solution. Then, take appropriate amounts of the standard solution to prepare a mixed standard solution, with the respective component concentrations being: Vitexin 49.0 μg/mL, Cannabiscitrin 42.7 μg/mL, Quercetin-3-O-α-arabinoside 1.9 μg/mL, Isovitexin 19.9 μg/mL, Quercetin 3-galactoside 0.9 μg/mL, and Apigenin 1.3 μg/mL. The above solutions are stored at 4 °C for future use. The standard curve is drawn with the reference peak area (Y) and the corresponding concentration (X) as the vertical and horizontal coordinates. The total flavonoid content was calculated using a standard curve. The limit of detection (LOD) and limit of quantitation (LOQ) were calculated with the signal-to-noise ratio (S/N) of 3 and 10 times, respectively.

The UPLC method was validated according to The International Council for Harmonization (ICH) guidelines [12], focusing on

Fig. 1. Fresh Jatropha leaves.

precision, accuracy, and linearity. Precision was evaluated using six independent test solutions, while intermediate precision was assessed by different analysts over three distinct days. Accuracy was determined through the recovery of standards from samples, with three varying quantities (low, medium, and high) of authentic standards added to a known real sample.

2.4. Animals and irradiation

Female Kunming mice, with an average weight of 20 ± 2 g, were acquired from the Animal Farm of the Sichuan Province Experimental Animal Special Commission. The radiation experiment was conducted at Zhongjin Radiation Chengdu Co., Ltd. The animals received humane care in accordance with the Guide for the Care and Use of Laboratory Animals, published by the U.S. National Institutes of Health (NIH publication, revised in 1985). Unanesthetized mice were individually placed in well-ventilated boxes and exposed to whole-body radiation of 8 Gy using ^{60}Co γ-rays. The radiation source was positioned 100 cm away, producing a dose rate of 1 Gy/min. The procedures and policies adhered to in conducting experiments on animals were duly approved by the Institutional Review Board (Ethics Committee) of Laboratory Animal Ethics Committee of Sichuan College of Traditional Chinese Medicine (2024DLKY002).

2.5. Determination of acute drug toxicity

Fasted animals were divided into two groups, each comprising 20 animals. In the experimental group, the animals received a freshly prepared extract of FEL at a dose of 0.2 mL per 10 g of body weight via intragastric administration. The control group was administered an equal volume of distilled water. The animals in the study received the treatments three times daily at a temperature range of 20–22 °C. Mortality rates and symptoms of poisoning were monitored for 14 days following drug administration. The drugs were weighed before and after 1 and 2 weeks, and the half-lethal dose (LD_{50}) of the extract was calculated. The maximum dose deemed suitable for the mice was determined to be 1700 mg/kg. Consequently, the administered dose of 400 mg/kg falls within the tolerance range for the mice.

2.6. Effect of FEL on radiation-induced mortality

Female mice were administered varying doses of FEL dissolved in distilled water over a duration of 21 days. The experimental mice were divided into seven groups, with one experimental group receiving Leucogen tablets (Jiangsu Jibeier Pharmaceutical Co., Ltd., 20 mg/piece) as their treatment. The control and model groups were administered distilled water. Mice in the FEL-1, FEL-2, FEL-3, and FEL-4 groups were intragastrically injected with 100, 200, 300, or 400 mg/kg of FEL per body weight per day, respectively. On day 7 following the administration of distilled water or FEL, all mice except those in the control group were exposed to whole-body radiation of 8 Gy γ-rays. These mice were monitored daily for the onset of radiation sickness symptoms and mortality.

2.7. Immunological indicators

2.7.1. Thymus index and spleen index

The animals were administered FEL at doses of 100, 200, 300, or 400 mg/kg prior to whole-body irradiation with 8 Gy. On day 14 post-irradiation, the mice were euthanized, and their spleens and thymuses were excised. The spleen and thymus indices were calculated by dividing the respective organ weights by the body weight, defined as: Thymus index=(thymus weight/BW) × 100 %, spleen index=(spleen weight/BW) × 100 % [13].

2.7.2. Peripheral blood cell count

0.2–0.3 mL eye blood samples were taken, and anticoagulant (disodium dihydrogen tetraacetate) was administered. The mixed blood samples were analyzed using the XN-2000 automatic blood cell analyzer (Sysmex, Japan). The recorded parameters included the number of white blood cells (WBC), red blood cells (RBC), platelets (PLT), hemoglobin (HGB), and lymphocytes (LY).

2.8. Splenic cell proliferation index

The animals were administered FEL at doses of 100, 200, 300, or 400 mg/kg body weight prior to whole-body irradiation with 8 Gy. On day 14 post-irradiation, the spleen was retrieved and placed on a 200-mesh screen, where it was ground until no visible red mass remained. Subsequently, the spleen was washed with 5 mL of phosphate-buffered saline (PBS). The spleen cell suspension was counted using trypan blue staining, and the splenic cells were enumerated under a microscope [14]. The cell suspension density was adjusted to 2×10^6 cells/ml, and 90 μl of this suspension was added to each well of a 96-well cell culture plate. Concanavalin A (Con A, 15 μg/well) powder was diluted to a 5 mg/mL solution using PBS, and then further diluted to a 15 μg/mL solution with RPMI 1640 medium. The experiments were repeated three times. The experimental group was treated with this solution, while the control group received RPMI 1640 medium. Cells were cultured at 37 °C in a 5 % CO_2 environment for 72 h. After 4 h, 5 mg/mL of methylthiazolyl tetrazolium (MTT) was added. Following the 72 h incubation, the cell suspension was treated with a 10 % aqueous solution of sodium dodecyl sulfate to completely dissolve the purple crystals. Optical density (OD) was measured at 570 nm using a microplate reader (318C+, Jingke, Shanghai). The proliferation index=(value for experimental well−value for the control well/value for control well) × 100 % [15].

2.9. Histological analysis

The liver sections from mice in each group were fixed in 10 % buffered formalin for 48 h and subsequently embedded in paraffin. The paraffin blocks were sectioned at 100 μm intervals, yielding two 4 μm slices from each block. The sections were stained with hematoxylin and eosin (H&E) and examined under an optical microscope.

2.10. Effect of FEL on micronucleus formation in the bone marrow

Animals were administered FEL at doses of 100, 200, 300, or 400 mg/kg body weight before exposure to 8 Gy of whole-body irradiation. The femoral heads of the mice were harvested on day 14. The samples were washed with 5 mL of PBS and centrifuged at 1200 rpm for 10 min. The supernatant was discarded, and the sediment was placed on a slide coated with serum. The smear was fixed in methanol fixative for 10 min and subsequently stained with Giemsa for 10 min. Micronuclei were detected in five evenly distributed fields of view, where mature erythrocytes appeared orange and polychromatic erythrocytes appeared blue when observed under a high-power microscope. Most micronuclei were round or oval, appearing as single or multiple entities with smooth, regular edges. The micronucleus rates (%) were determined by counting the number of micronuclei present in 1000 polychromatic erythrocytes.

2.11. Effect of FEL on the DNA quantity in the bone marrow

Bone marrow was extracted from the femur by flushing with 10 mL of calcium chloride solution (5 mmol/L) and collected in refrigerated centrifuge tubes at 4 °C for 30 min. Subsequently, the samples were centrifuged at 2500 rpm for 15 min. The supernatant was removed, and 5 mL of perchloric acid was added to the sediment, which was heated at 90 °C for 15 min. After cooling, the supernatant was obtained by centrifugation at 3500 rpm for 10 min. The optical density (OD) was measured at 268 nm using a UV spectrophotometer (UV-2401PC, Shimadzu Corporation, Japan). DNA content (μg) = 40 × 50 A (absorbance) [16].

2.12. Protective effect of FEL on DNA in mouse hepatocytes

The comet assay (single-cell gel electrophoresis) was employed to quantify oxidative DNA damage induced by hydrogen peroxide in mouse hepatocytes [17]. Following modification, the single-cell suspension was combined with 100 μL of 0.5 % low melting point

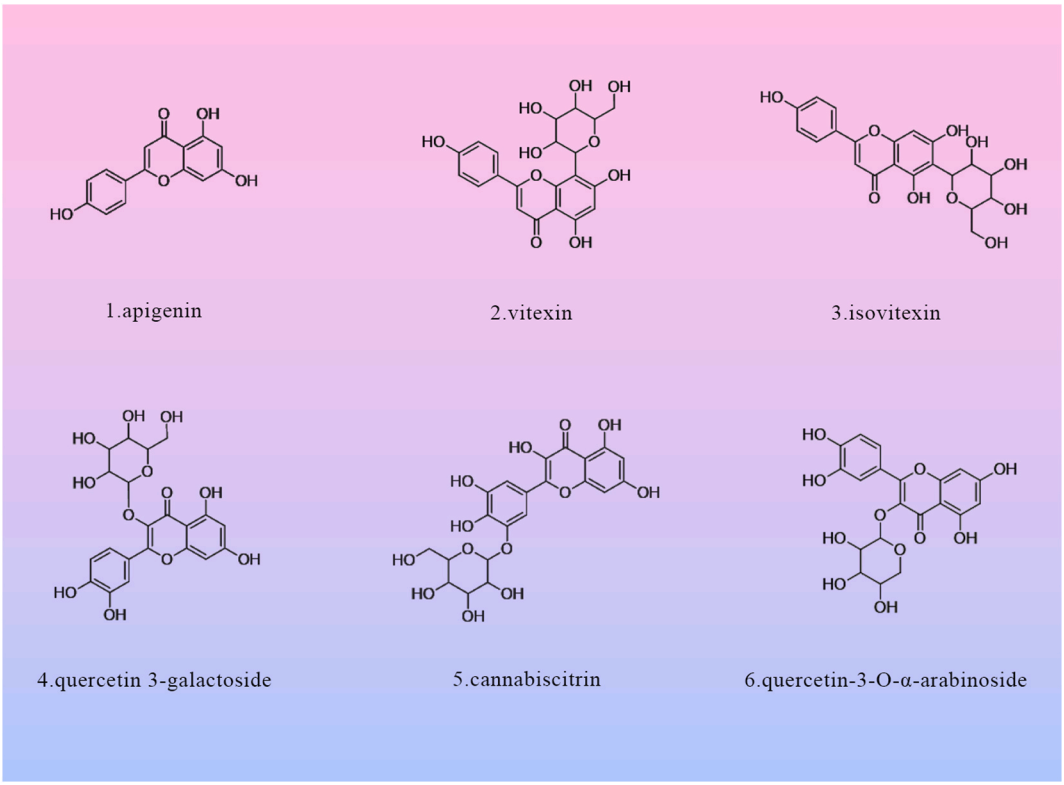

Fig. 2. The 6 chemical structures of FEL.

agarose (NMPA, Biotechnology, Japan). Subsequently, the cells were layered onto frosted microscope slides pre-coated with low melting point agarose and dispersed using additional low melting point agarose. The slides were incubated in a 4 °C lysis buffer for 90 min before undergoing electrophoresis (DYC 34A Liuyi Instrument Station, Beijing) at 25 V and 300 mA for 20 min in an alkaline buffer solution (300 mM NaOH, 1 mM EDTA, pH 13). Following three washes, the slides were counterstained with 100 μL of ethidium bromide and observed under a fluorescence microscope (BX 51, Olympus, Japan). Quantification of DNA strand breaks was performed using the Komet 5.5 procedure by Kinetic Imaging (Liverpool, UK). This method enables direct assessment of DNA content, tail length, and damage rate within the comet tail.

2.13. Statistical analysis

Each treatment was replicated a minimum of three times, and the results are presented as mean ± standard deviation (SD). Statistical significance was assessed using a paired *t*-test, with significance levels set at $P < 0.05$ or $P < 0.01$.

3. Results

3.1. Analysis of the chemical profile of FEL

The content of FEL in the extracted and purified yellow powder was 1.1 % (w/w). The chemical spectra of FEL were analyzed, focusing on six specific flavonoids: Apigenin, Vitexin, Isovitexin, Quercetin 3-galactoside, Cannabiscitrin, and Quercetin-3-O-α-arabinoside (Fig. 2).

The sample was positioned on the sample plate of the UPLC system and automatically injected to produce the UPLC chromatogram (Fig. 3). Characterization of active constituents was carried out by cospiking with standard markers and by UPLC. The results of methodology investigation on FEL were shown in Table 1. The results indicated a strong linear relationship among the standard samples. Quercetin 3-galactoside accounted for approximately 10 % of the FEL, while total flavonoids comprised 78 %.

The recovery rates for the analyzed components ranged from 96.4 % to 101.7 %, with all relative standard deviation (RSD) values remaining below 5.0 %. These results indicate that the method demonstrates both high reliability and accuracy.

3.2. Acute toxicity

During the entire observation period, there were no instances of mortality associated with FEL administration, despite a slight decrease in activity. All physiological parameters—including appearance, respiration, heart rate, appetite, weight, and excretion—remained within normal ranges throughout the study. Postmortem examinations showed no pathological changes. Based on these findings, it was concluded that FEL administration did not result in mortality. The maximum dosage of FEL established for mice was 1700 mg/kg.

3.3. Effect of FEL on survival rate of irradiated mice

Exposure to ^{60}Co γ-rays through total body irradiation at a dose of 8 Gy reduced the survival rate of the mice to 65 % after 21 days, underscoring the detrimental effects of radiation on their health. Additionally, irradiation was associated with a decrease in appetite and reduced activity levels. In the FEL group, the survival rate exceeded that of the untreated group and displayed a dose-dependent pattern, with the high-dose group achieving a 100 % survival rate (see Table 2). These findings suggest that FEL confers protective benefits against the harmful effects of gamma radiation.

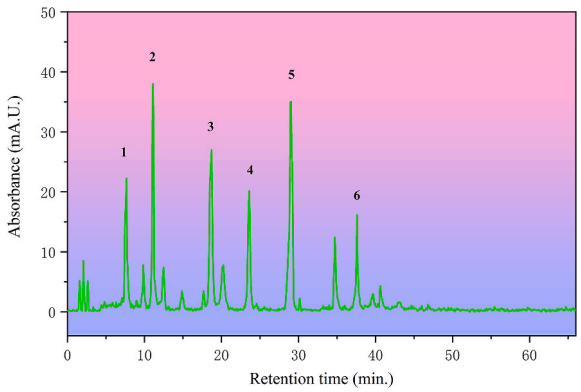

Fig. 3. UPLC spectrum of FEL.

Table 1
Results of methodology investigation on FEL.

Compont	Linear equation	R^2	Linear range/(μg·mL^{-1})	LOD/(μg·mL^{-1})	LOQ/(μg·mL^{-1})
Apigenin	Y = 578.2X+3.4908	1.0000	0.0064-1.2717	0.09	0.29
Vitexin	Y = 3261.9X+1928.8	0.9990	0.2452-49.0447	0.57	1.91
Isovitexin	Y = 7916.4X+2129.1	0.9993	0.0997-19.9367	0.16	0.55
Quercetin 3-galactoside	Y = 2698.1X+19.246	0.9994	0.0044-0.8891	0.03	0.11
Cannabiscitrin	Y = 2401.9X+2990.9	0.9995	0.2136-42.7217	0.38	1.26
Quercetin-3-O-α-arabinoside	Y = 4095X+55.215	0.9997	0.0095-1.9050	0.06	0.21

3.4. Effects of FEL on immune function

Mice subjected to total-body irradiation with 8 Gy of ^{60}Co γ-rays exhibited a significant reduction in both thymus and spleen indices ($P < 0.01$). Notably, the thymus index of the FEL-4 and FEL-3 groups was significantly higher than that of the Leucogen group ($P < 0.01$). As shown in Fig. 4A, the spleen indices of the FEL-4, FEL-3, and FEL-2 groups were markedly elevated compared to the Leucogen group ($P < 0.01$). These results suggest that FEL exerts a protective effect by increasing the weight of immune organs. Furthermore, as illustrated in Fig. 4B, the proliferation indices of T-cells and B-cells in all FEL-treated irradiated groups demonstrated a significant increase in a dose-dependent manner compared to the model group ($P < 0.05$). These results suggest that FEL enhances splenic lymphocyte proliferation.

3.5. Influence of FEL on peripheral blood cell count

Mice treated with FEL exhibited significantly elevated levels of WBC, RBC, PLT, and HGB damage compared to the unirradiated normal group ($P < 0.05$, $P < 0.01$). However, there was no significant decrease in LY ($P > 0.05$). Compared to the model group, WBC, RBC, PLT, LY, and HGB counts in the FEL-4, FEL-3, and FEL-2 groups were elevated, with statistically significant differences observed in WBC, RBC, LY, and HGB counts ($P < 0.05$), while the differences in PLT count were not significant ($P > 0.05$). This lack of significance may be attributed to the effects of radiation on bone marrow progenitor cells and the short lifespan of blood cells. No significant difference was found in blood cell counts between the FEL-1 group and the model group ($P > 0.05$). The peripheral blood cell count in the Leucogen group was comparable to that in the FEL-2 group, while the FEL-3 group was similar to the FEL-4 group (see Table 3). These results suggest that FEL could reduce the effects of radiation on hemograms in mice.

3.6. Influence of FEL on pathological changes of liver tissue damaged by radiation

Hepatic cords of normal liver tissue were arranged in an orderly fashion, with hepatic sinuses showing neither hyperemia nor enlargement. Hepatocytes exhibited no edema, degeneration, or necrosis; the central vein wall remained intact, and the lumen was neither enlarged nor obstructed. Additionally, there was no collagen fiber deposition around the central vein (see Fig. 5A). In the radiation model group, numerous dark and distorted cell nuclei were observed, and hepatocytes exhibited pronounced edema and degeneration, accompanied by noticeable inflammatory cell infiltration around the central vein. Furthermore, there was an increase in surrounding reticular fibers, leading to their constriction and obstruction (see Fig. 5B). In the Leucogen group, no significant reduction in collagen fiber deposition around the central vein wall was observed (see Fig. 5C), and the cell shape appeared predominantly normal, similar to that in the FEL-4 group (see Fig. 5G). In the FEL-1 group, there was a slight decrease in inflammatory cell infiltration and peripheral reticular fibers; however, edema and necrosis remained evident (see Fig. 5D). Subsequently, both edema and necrosis were further diminished in the FEL-2 and FEL-3 groups (see Fig. 5E and F).

Table 2
Statistical effect of FEL on survival rate of irradiated mice.

Group	Dose(mg/kg)	n	Survival number(n)	Survival rate(%)	Average survival days
Normal	–	20	20	100	21.00 ± 0.00
Model	–	20	13	65	19.73 ± 5.69*
Leucogen	1.4	20	17	85	20.68 ± 2.32◆
FEL-1	100	20	16	80	20.35 ± 5.39
FEL-2	200	20	17	85	20.61 ± 4.65
FEL-3	300	20	19	95	20.82 ± 2.17◆
FEL-4	400	20	20	100	21.00 ± 0.00◆

A total of 140 mice underwent daily intragastric administration of FEL for 21 consecutive days. On the seventh day, all groups, except the normal group, were subjected to 8 Gy of whole-body γ-ray radiation. The mice were subsequently monitored daily for signs of radiation sickness and mortality. Statistical significance was indicated by the following symbols: * for comparisons with the normal group ($P < 0.05$) and ◆ for comparisons with the model group ($P < 0.05$).

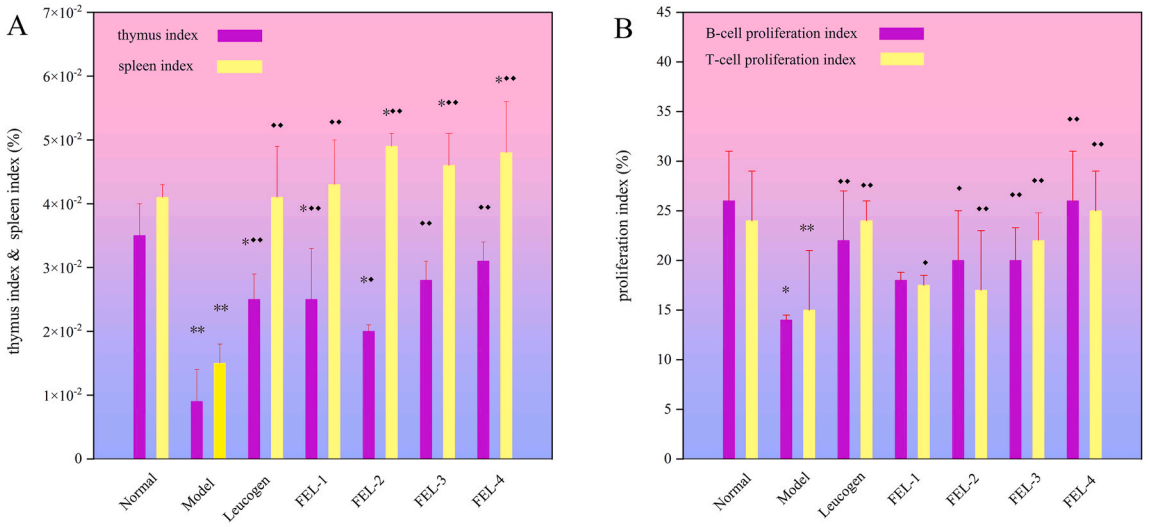

Fig. 4. Effects of FEL on Immune Function. (A) The impact of FEL on thymus and spleen indices was evaluated following oral administration. After a 7-day treatment period, 60 mice were exposed to ^{60}Co γ-rays and subsequently sacrificed on day 14 for the measurement of spleen and thymus parameters. The reported values represent the SD derived from 10 independent experiments. (B) The effect of FEL on lymphocyte proliferation was investigated by surgically removing spleens from seven groups of mice under aseptic conditions. Spleen cells were cultured in 96-well plates for 72 h with ConA, and absorbance was quantified using an enzyme-linked method. Statistically significant differences were indicated by the following symbols: * for $P < 0.05$, ** for $P < 0.01$ compared to the normal group, and ◆ for $P < 0.05$, ◆◆ for $P < 0.01$, compared to the model group.

Table 3
Statistical effects of FEL on peripheral blood cell count in mice.

Group	Dose (mg/kg)	n	WBC (× 10^9/L)	RBC (× 10^{12}/L)	PLT (× 10^{12}/L)	LY (%)	HGB (g/L)
Normal	–	11	7.12 ± 2.38	7.36 ± 0.23	1053.11 ± 221.83	76.81 ± 6.43	145.42 ± 7.47
Model	–	13	2.07 ± 0.98**	5.97 ± 0.78**	896.04 ± 214.12*	74.39 ± 13.31	118.01 ± 19.22**
Leucogen	1.4	11	2.88 ± 1.31**	6.47 ± 0.99*	891.71 ± 76.25*	72.55 ± 15.85	124.05 ± 11.82*
FEL-1	100	12	2.58 ± 1.12**	6.23 ± 0.76*	867.70 ± 134.65	62.79 ± 5.32*	126.5 ± 13.04*
FEL-2	200	12	2.73 ± 1.12**	6.52 ± 0.75*	872.43 ± 156.52*	60.38 ± 16.78*◆	129.82 ± 8.37*
FEL-3	300	11	3.44 ± 1.43**	6.68 ± 0.85*◆	943.23 ± 178.14*	73.45 ± 10.65*◆	131.31 ± 9.98*◆
FEL-4	400	11	3.73 ± 0.96**◆	6.78 ± 1.02*◆	988.14 ± 213.82	77.03 ± 6.79*◆	134.21 ± 11.37*◆

FEL was administered intragastrically to 70 mice once daily for 14 consecutive days. On day 7, all mice, except for those in the normal group, were exposed to 8 Gy of whole-body γ-ray radiation. The alterations in peripheral blood cell parameters were assessed on day 14. Statistically significant differences were denoted by the following symbols: * for $P < 0.01$ and ** for $P < 0.05$ compared to the normal group, and ◆ for $P < 0.05$ in comparison to the model group.

3.7. Effect of FEL on micronucleus formation in mouse bone marrow

Irradiation significantly increased the incidence of micronuclei in the bone marrow ($P < 0.01$). The micronucleus rate in the bone marrow of the FEL-2, FEL-3, FEL-4, and Leucogen groups was notably lower than that in the model group ($P < 0.01$). The bone marrow micronucleus rate of the FEL-1 group was comparable to that of the model group ($P > 0.05$) (see Table 4). These results suggest that elevated doses of FEL suppress the production of radiation-induced micronuclei.

3.8. Effect of FEL on DNA quantity in mouse bone marrow

Whole-body irradiation resulted in a substantial decrease in DNA content in the mouse bone marrow ($P < 0.01$). Conversely, the bone marrow DNA content in the FEL-4, FEL-3, and Leucogen groups exhibited significant elevations compared to the model group ($P < 0.01$, $P < 0.01$, and $P < 0.05$, respectively). The DNA content in the bone marrow of the FEL-1 and FEL-2 groups was greater than that in the model group; however, this variance lacked statistical significance ($P > 0.05$) (see Fig. 6).

3.9. Protective effect of FEL against DNA in mouse hepatocytes

The results of single-cell gel electrophoresis demonstrate that the injury rate of mouse hepatocytes in the model group nearly reached 100 %, indicating severe DNA damage. The extent of injury in hepatocytes of the Leucogen group was slightly greater than that of the FEL-4 group. The extent of injury in the hepatocytes of the FEL-1 group resembled that of the model group. However, as the

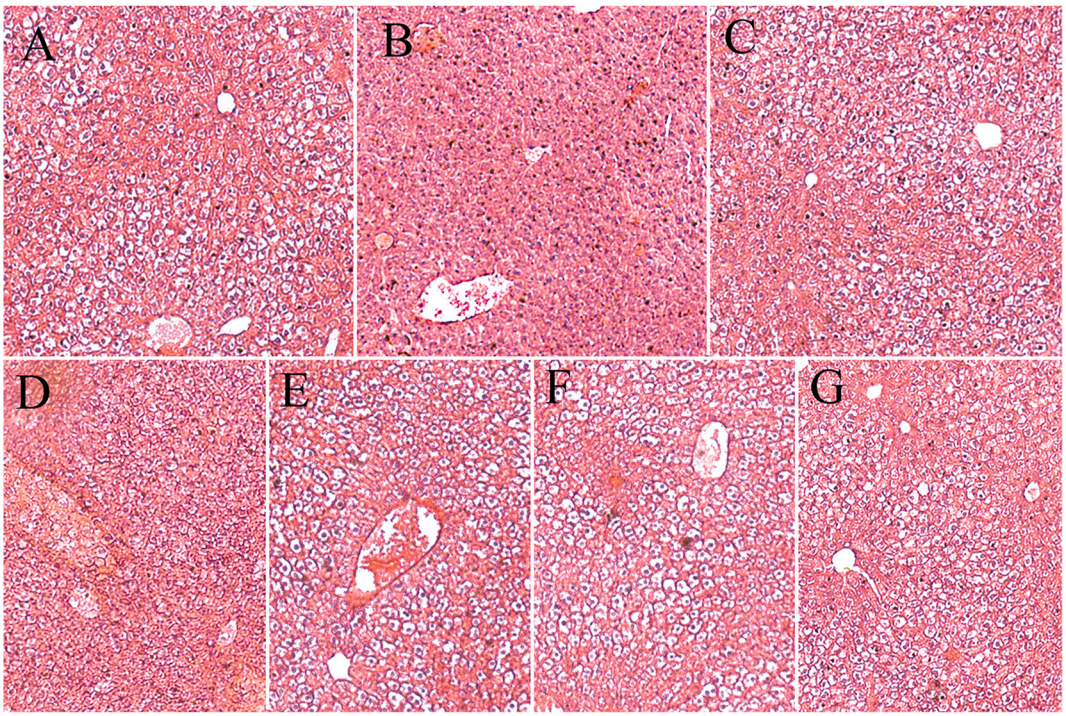

Fig. 5. Morphological Changes in Radiation-Damaged Mouse Liver (H&E, × 80). A total of 70 tissue sections were divided into seven groups and fixed in 10 % buffered formalin for several hours. After overnight incubation, the slices were embedded in paraffin. Subsequently, the blocks were cut at 100 μm intervals, and two 4 μm slices were obtained from each group. The sections were then stained with HE. (A) normal control group; (B) model group; (C) Leucogen treatment group; (D, E, F, G) FEL-1 group, FEL-2 group, FEL-3 group, and FEL-4 group, respectively.

Table 4
Statistical effects of FEL on peripheral blood cell count in mice.

Group	Dose(mg/kg)	n	Micronuclear rates (‰)
Normal	–	11	11.00 ± 6.00
Model	–	13	24.88 ± 6.88**
Leucogen	1.4	11	20.00 ± 8.00**◆◆
FEL-1	100	12	22.14 ± 4.14**
FEL-2	200	12	20.56 ± 5.56**◆◆
FEL-3	300	11	18.87 ± 4.42**◆◆
FEL-4	400	11	18.13 ± 4.13**◆◆

FEL was administered once daily for 14 consecutive days. Following the exclusion of the normal control group, 70 mice were subjected to whole-body irradiation with 8 Gy of ^{60}Co γ-rays on day 7. Bone marrow fluid was extracted from the femur heads of the mice, and smears were examined under a high-power microscope. Statistical analysis was performed by comparing measurements taken on various days post-irradiation. Statistically significant differences were denoted by the following symbols: ** for $P < 0.01$ when compared to the normal group and ◆◆ for $P < 0.01$ when compared to the model group.

concentration of FEL increased, the damage rate steadily decreased, accompanied by reductions in tail DNA and tail head ratios (see Fig. 7). These findings suggest that FEL exhibited a radioprotective effect in mouse hepatocytes.

4. Discussion

Radiation is a significant contributor to physical harm, particularly immune impairment. It can induce cells to initiate an oxidative stress response through the generation of reactive oxygen species. Fruits, vegetables, nuts, seeds, tea, and wine are abundant sources of flavonoids. While previous research has demonstrated the potential of flavonoids to mitigate radiation-induced damage, the specifics of their radioprotective effects remain unclear [18,19].

FEL is a commonly used and readily available ingredient in herbal formulations. It provided optimal protection against mortality in whole-body irradiated mice at doses of up to 400 mg/kg. However, increasing the drug dosage beyond this point did not enhance survival rates and showed no further dose dependency. This study demonstrates that FEL exhibits protective effects on hematopoietic tissues and the immune system, resulting in a substantial improvement in the survival rate of irradiated mice.

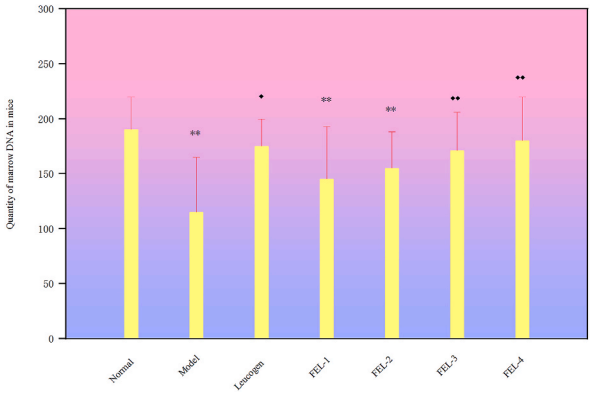

Fig. 6. The impact of FEL on DNA quantity in mouse bone marrow was assessed. Perchloric acid was introduced to seven groups of 81 bone marrow samples and heated at 90 °C for 15 min. Subsequently, the optical densities were measured using a UV spectrophotometer at 268 nm. Statistically significant differences were denoted by the following symbols: ** for $P < 0.01$ compared to the normal group, and ◆ for $P < 0.05$, ◆◆ for $P < 0.01$ in comparison with the model group.

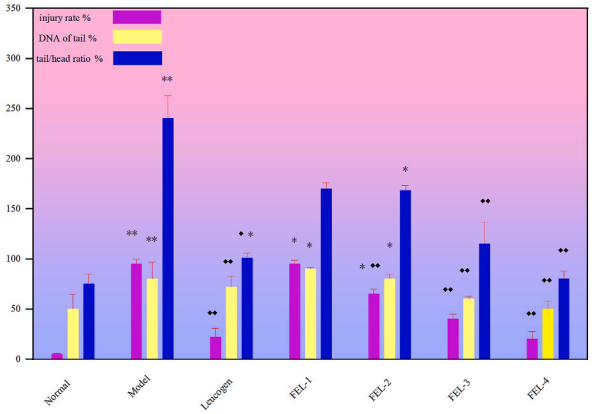

Fig. 7. Single-cell gel electrophoresis (comet assay) was used to assess the protective effect of FEL against DNA damage (× 200). The age rate, tail DNA, and tail head ratios were calculated and examined. Statistical analysis included comparisons of measurements taken on various days following irradiation. Significant differences were denoted by the following symbols: * for $P < 0.05$, ** for $P < 0.01$ compared to the normal group, and ◆ for $P < 0.05$, ◆◆ for $P < 0.01$ relative to the model group.

Hematopoietic tissues and the immune system are highly vulnerable to radiation. Suppression of hematopoiesis is a significant clinical manifestation of radiation-induced damage to the hematopoietic system, primarily caused by a reduction in the proliferative capacity of hematopoietic stem cells. Low-dose radiation-induced acute damage typically correlates with immune system disorders and is accompanied by reductions in both white blood cell and red blood cell counts [20]. The results of the current study indicate that FEL increased levels of WBC, RBC, PLT, HGB, and LY in the peripheral blood of irradiated mice, thereby enhancing hematopoietic function and overall survival rates.

T lymphocytes are particularly vulnerable to radiation exposure. Typically, radiation suppresses the immune system by inhibiting bone marrow function, reducing immune cell counts, inducing microcirculatory disturbances, decreasing interleukin production, and impairing the microenvironment [21]. Therefore, treating the immune system is crucial for managing radiation-related ailments. The results of the current study indicate that FEL significantly enhanced lymphocyte transformation stimulated by Con A, potentially leading to protective effects on the thymus and spleen. This study demonstrates that FEL can bolster immunity, aligning with findings from previous studies [22].

In both normal tissues and tumors, the primary mechanism of radiation-induced damage involves oxidative damage to DNA caused by free radicals. This damage can manifest as single-strand breaks, double-strand breaks, base damage, and cross-linked DNA damage, ultimately leading to apoptosis or cell death. Ionizing radiation can directly affect nucleic acids, proteins, and enzymes by inducing ionization or breaking chemical bonds, resulting in the degradation of molecular structures and cellular damage. Radiation damage at the molecular level impacts the bone marrow, leading to chromosomal aberrations and an increased presence of micronuclei [23]. Micronucleus detection serves as a critical indicator of radiation damage, accurately reflecting the extent of chromosome damage and the efficacy of repair mechanisms. The bone marrow micronucleus rates obtained in this experiment demonstrated that FEL significantly reduced DNA damage. Furthermore, FEL treatment markedly increased bone marrow DNA content, providing additional

evidence of FEL's protective effect on DNA.

Radiation-induced damage predominantly arises from the overproduction of reactive species such as the superoxide anion radical, hydroxyl radical, and H_2O_2. When the generation of reactive oxygen species exceeds the antioxidant capacity, it leads to oxidative stress, cellular damage, and DNA strand breaks. The comet assay (single-cell gel electrophoresis) is a reliable method for detecting DNA damage, repair, and apoptosis at the individual cell level. The presence of a comet is indicative of DNA breakage, with the shape of the comet reflecting both the extent and nature of the DNA damage.

This study examined the impact of FEL on DNA damage caused by the oxidation of mouse hepatocytes by evaluating non-specific DNA damage at the genome-wide level. Mouse hepatocyte cells treated with H_2O_2 exhibited significant DNA damage. At the highest FEL dose (400 mg/kg), there was a gradual reduction in the occurrence of radiation-induced DNA damage, decreasing from 95.13 % to 19.82 %. This protective mechanism may be associated with cellular integrity, safeguarding the nucleus from radiation damage by stabilizing membrane fluidity or reducing permeability.

5. Conclusions

FEL provides protection against radiation and oxidative damage to the body. Furthermore, the radiation-protective mechanism of FEL is associated with enhanced immune function and the safeguarding of the hematopoietic system. These findings support the notion of considering FEL as a potential clinical anticancer agent.

CRediT authorship contribution statement

Qinling Li: Writing – original draft, Supervision, Investigation, Project administration, Data curation, Visualization, Formal analysis. **Dan He:** Writing – review & editing, Methodology, Validation, Resources, Formal analysis. **Yang He:** Writing – review & editing, Methodology, Validation, Resources, Formal analysis.

Ethics statements

The experiments conducted on animals adhered strictly to the procedures and policies approved by the Institutional Review Board (Ethics Committee) of Laboratory Animal Ethics Committee of Sichuan College of Traditional Chinese Medicine (Approval No. 2024DLKY002).

Funding

This research received no external funding.

Declaration of competing interest

The authors declare that they have no known competing financial interests or personal relationships that could have appeared to influence the work reported in this paper.

List of Abbreviations

FEL	Flavonoids Extracted from Jatropha curcas Leaves
UPLC	Ultra Performance Liquid Chromatography
ICH	International Council for Harmonization
LD50	half-lethal dose
WBC	white blood cells
RBC	red blood cells
PLT	platelets
HGB	hemoglobin
LY	lymphocytes
PBS	phosphate-buffered saline
Con A	Concanavalin A
MTT	methylthiazolyl tetrazolium
OD	Optical density
H&E	hematoxylin and eosin
SD	standard deviation
RSD	relative standard deviation

Data availability statement

Data will be made available on request.

References

[1] A.B. Heeran, H.P. Berrigan, J. O'Sullivan, The radiation-induced bystander effect (RIBE) and its connections with the hallmarks of cancer, Radiat. Res. 192 (2019) 668, https://doi.org/10.1667/rr15489.1.

[2] V. Schirrmacher, From chemotherapy to biological therapy: a review of novel concepts to reduce the side effects of systemic cancer treatment, Int. J. Oncol. 54 (2017) 407–419, https://doi.org/10.3892/ijo.2018.4661 (Review).

[3] B.P. Jit, S. Pattnaik, R. Arya, R. Dash, S.S. Sahoo, B. Pradhan, P.P. Bhuyan, P.K. Behera, M. Jena, A. Sharma, P.K. Agrawala, R.K. Behera, Phytochemicals: a potential next generation agent for radioprotection, Phytomedicine 106 (2022) 154188, https://doi.org/10.1016/j.phymed.2022.154188.

[4] T. Li, Y. Cao, B. Li, R. Dai, The biological effects of radiation-induced liver damage and its natural protective medicine, Prog. Biophys. Mol. Biol. 167 (2021) 87–95, https://doi.org/10.1016/j.pbiomolbio.2021.06.012.

[5] Y. Zhang, Y. Huang, L. Zheng, H. Wu, B. Zou, Y. Xu, Exploring natural products as radioprotective agents for cancer therapy: mechanisms, challenges, and opportunities, Cancers 15 (2023), https://doi.org/10.3390/cancers15143585, 3585–3585.

[6] J. Shi, J. Guo, L. Chen, L. Ding, H. Zhou, X. Ding, J. Zhang, Characteristics and anti-radiation activity of different molecular weight polysaccharides from Potentilla anserina L, J. Funct.Foods 101 (2023) 105425, https://doi.org/10.1016/j.jff.2023.105425.

[7] A. Stasiłowicz-Krzemień, A. Gościniak, Dorota Formanowicz, Judyta Cielecka-Piontek, Natural Guardians, Natural compounds as radioprotectors in cancer therapy, Int. J. Mol. Sci. 25 (2024), https://doi.org/10.3390/ijms25136937, 6937–6937.

[8] Y.C. Vega-Ruiz, C. Hayano-Kanashiro, N. Gámez-Meza, L.A. Medina-Juárez, Determination of chemical constituents and antioxidant activities of leaves and stems from Jatropha cinerea (ortega) Müll. Arg and Jatropha cordata (Ortega) Müll, Arg, Plants 10 (2021) 212, https://doi.org/10.3390/plants10020212.

[9] N.B. Cavalcante, A. Diego da Conceição Santos, J.R. Guedes da Silva Almeida, The genus Jatropha (Euphorbiaceae): a review on secondary chemical metabolites and biological aspects, Chem. Biol. Interact. 318 (2020) 108976, https://doi.org/10.1016/j.cbi.2020.108976.

[10] M. Aurélio, A. Júnio, Hamilton Hisano, Growth, metabolism and digestibility of Nile tilapia fed diets with solvent and extrusion-treated Jatropha curcas cake, Vet. Res. Commun. 47 (2023) 1273–1283, https://doi.org/10.1007/s11259-023-10076-3.

[11] W.L.F. Dias, E.P. do Vale Junior, M. das Dores Alves de Oliveira, Y.L.P. Barbosa, J. do Nascimento Silva, J.S. da Costa Júnior, P.M. de Almeida, F.A. Martins, Cytogenotoxic effect, phytochemical screening and antioxidant potential of Jatropha mollissima (Pohl) Baill leaves, South Afr. J. Bot. 123 (2019) 30–35, https://doi.org/10.1016/j.sajb.2019.02.007.

[12] A. Pawar, N. Pandita, Statistically Designed, targeted profile UPLC method development for assay and purity of haloperidol in haloperidol drug substance and haloperidol 1 mg tablets, Chromatographia 83 (2020) 725–737, https://doi.org/10.1007/s10337-020-03889-w.

[13] K.-Y. Liu, I-Pei Kuo, Y.-J. Chen, P.-T. Lee, C.-J. Lee, Oral administration of tilapia hydrolysate peptides ameliorates the immune-related side effects of cyclophosphamide in BALB/c mice, Food Biosci. 56 (2023), https://doi.org/10.1016/j.fbio.2023.103428, 103428–103428.

[14] S. Sutradhar, A. Deb, S.S. Singh, Melatonin attenuates diabetes-induced oxidative stress in spleen and suppression of splenocyte proliferation in laboratory mice, Arch. Physiol. Biochem. 128 (2020) 1–12, https://doi.org/10.1080/13813455.2020.1773506.

[15] M. Faghani, S. Saedi, K. Khanaki, F. Mohammadghasemi, Ginseng alleviates folliculogenesis disorders via induction of cell proliferation and downregulation of apoptotic markers in nicotine-treated mice, J. Ovarian Res. 15 (2022) 14, https://doi.org/10.1186/s13048-022-00945-x.

[16] K. Reinmuth-Selzle, T. Tchipilov, A.T. Backes, G. Tscheuschner, K. Tang, K. Ziegler, K. Lucas, U. Pöschl, J. Fröhlich-Nowoisky, M.G. Weller, Determination of the protein content of complex samples by aromatic amino acid analysis, liquid chromatography-UV absorbance, and colorimetry, Anal. Bioanal. Chem. 414 (2022) 4457–4470, https://doi.org/10.1007/s00216-022-03910-1.

[17] S. Choudhury, A.Y. Huang, J. Kim, Z. Zhou, K. Morillo, E.A. Maury, J.W. Tsai, M.B. Miller, M.A. Lodato, S. Araten, N. Hilal, E.A. Lee, M.H. Chen, C.A. Walsh, Somatic mutations in single human cardiomyocytes reveal age-associated DNA damage and widespread oxidative genotoxicity, Nature Aging 2 (2022) 714–725, https://doi.org/10.1038/s43587-022-00261-5.

[18] S. Wu, C. Tian, Z. Tu, J. Guo, F. Xu, W. Qin, H. Chang, Z. Wang, T. Hu, X. Sun, H. Ning, Y. Li, W. Gou, W. Hou, Protective effect of total flavonoids of Engelhardia roxburghiana Wall. leaves against radiation-induced intestinal injury in mice and its mechanism, J. Ethnopharmacol. 311 (2023), https://doi.org/10.1016/j.jep.2023.116428, 116428–116428.

[19] Shamprasad Varija Raghu, S. Rao, V. Kini, Avinash Kundadka Kudva, T. George, Manjeshwar Shrinath Baliga, Fruits and their phytochemicals in mitigating the ill effects of ionizing radiation: review on the existing scientific evidence and way forward, Food Funct. 14 (2023) 1290–1319, https://doi.org/10.1039/d2fo01911f.

[20] S.O. Sowemimo-Coker, L.D. Fast, Effects of hypoxic storage on the efficacy of gamma irradiation in abrogating lymphocyte proliferation and on the quality of gamma-irradiated red blood cells in additive solution 3, Transfusion 61 (2021) 3443–3454, https://doi.org/10.1111/trf.16683.

[21] J. Cadet, D. Angelov, J.R. Wagner, Hydroxyl radical is predominantly involved in oxidatively generated base damage to cellular DNA exposed to ionizing radiation, Int. J. Radiat. Biol. (2022) 1–7, https://doi.org/10.1080/09553002.2022.2067363.

[22] L.M. Davidovic, D. Laketic, J. Cumic, E. Jordanova, I. Pantic, Application of artificial intelligence for detection of chemico-biological interactions associated with oxidative stress and DNA damage, Chem. Biol. Interact. 345 (2021) 109533, https://doi.org/10.1016/j.cbi.2021.109533.

[23] Ganesh Chandra Jagetia, Antioxidant activity of curcumin protects against the radiation-induced micronuclei formation in cultured human peripheral blood lymphocytes exposed to various doses of γ-Radiation, Int. J. Radiat. Biol. 97 (2021) 485–493, https://doi.org/10.1080/09553002.2021.1876948.